

## A stochastic model for daily subsurface CO<sub>2</sub> concentration and related soil respiration

Edoardo Daly<sup>a,b,c,\*</sup>, A. Christopher Oishi<sup>b</sup>, Amilcare Porporato<sup>a,b</sup>, Gabriel G. Katul<sup>b,a</sup>

<sup>a</sup> Department of Civil and Environmental Engineering, Duke University, Durham, NC, USA

<sup>b</sup> Nicholas School of the Environment and Earth Sciences, Duke University, Durham, NC, USA

<sup>c</sup> Department of Civil Engineering, Monash University, Building 60, Clayton Campus, Clayton, VIC 3800, Australia

### ARTICLE INFO

#### Article history:

Received 4 December 2007

Received in revised form 25 March 2008

Accepted 2 April 2008

Available online 8 April 2008

#### Keywords:

Soil CO<sub>2</sub>

CO<sub>2</sub> pulses

Soil respiration

Rainfall

### ABSTRACT

Near-surface soil CO<sub>2</sub> gas-phase concentration ( $C$ ) and concomitant incident rainfall ( $P_i$ ) and through-fall ( $P_t$ ) depths were collected at different locations in a temperate pine forest every 30 min during the 2005 and 2006 growing seasons (and then averaged to the daily timescale). At the daily scale,  $C$  temporal variations were well described by a sequence of monotonically decreasing functions interrupted by large positive jumps induced by rainfall events. A stochastic model was developed to link rainfall statistics responsible for these jumps to near-surface  $C$  dynamics. The model accounted for the effect of daily rainfall variability, both in terms of timing and amount of water, and permitted an analytical derivation of the  $C$  probability density function (pdf) using the parameters of the rainfall pdf. Given the observed positive correlation between daily  $C$  and soil CO<sub>2</sub> fluxes to the atmosphere ( $F_s$ ), the effects of various rainfall regimes on the statistics of  $F_s$  can be deduced from the behavior of  $C$  under different climatic conditions. The predictions from this analytical model are consistent with flux measurements reported in manipulative experiments that varied rainfall amount and frequency.

© 2008 Elsevier Ltd. All rights reserved.

### 1. Introduction

Soil CO<sub>2</sub> fluxes ( $F_s$ ) to the atmosphere are the result of complex physical and biological processes that depend on soil properties, vegetation and microbial characteristics, and climatic conditions [12,29]. In particular, the effects of environmental fluctuations on  $F_s$ , such as the rapid fluctuations in soil moisture and temperature or the slow increase in atmospheric CO<sub>2</sub> concentration and nitrogen deposition, remain the subject of active research [10,13,21,22,32,46].

Soil respiration pulses following rainfall events have been observed in several ecosystems [15,36,44,47]. The importance of these pulses on annual respiration appears to vary across ecosystems. Lee et al. [42] found that post-rainfall increases in  $F_s$  might represent approximately 16–21% of the annual soil carbon flux in a cool temperate deciduous forest in Japan, while the estimates of Lee et al. [43] in a mixed forest in Connecticut (USA) were between 5% and 10%. Xu et al. [62] suggested that soil carbon losses by rainfall pulses might be comparable to annual net ecosystem carbon dioxide exchange in many terrestrial ecosystems, especially

for arid and semiarid ones. A manipulative experiment in a grassland ecosystem, described in Knapp et al. [40] and Harper et al. [30], concluded that  $F_s$  is not only dependent on precipitation amounts but also on the frequency of rainfall occurrence. These findings open new questions on how changes in rainfall patterns modify soil respiratory components.

This study is guided by the strong relationship between CO<sub>2</sub> fluxes and subsurface CO<sub>2</sub> concentrations,  $C$ , which now can be monitored at unprecedented time resolution using solid-state infrared gas analyzers [60]. When taken together, how the dynamics of  $C$  is impacted by pulsed rainfall, and the consequences of this rainfall intermittency on the dynamics of CO<sub>2</sub> fluxes from the soil to the atmosphere can now be explored.

Numerous and complex interconnections between the physical and biological processes occur in the soil during and after rainfall events. During precipitation, water infiltration displaces an equivalent volume of air thereby enhancing air-phase CO<sub>2</sub> fluxes [29]. However, rainfall also reduces CO<sub>2</sub> fluxes because of the reduction in gas-phase soil CO<sub>2</sub> diffusivity ( $D$ ). In fact, the increase in soil water content following rainfall events significantly reduces  $D$  thus favoring the build-up of higher CO<sub>2</sub> concentration levels [15,29,36] even if the CO<sub>2</sub> production remains unaltered. In addition to these physical effects, increased soil moisture levels can enhance microbial activity [5,35,45] by two mechanisms. The first is through the mineralization of non-biomass soil organic carbon, which becomes readily accessible to microbial attack following soil aggregate

\* Corresponding author. Address: Department of Civil Engineering, Monash University, Building 60, Clayton Campus, Clayton, VIC 3800, Australia. Tel.: +61 3 9905 4979; fax: +61 3 9905 4944.

E-mail addresses: [Edoardo.Daly@eng.monash.edu.au](mailto:Edoardo.Daly@eng.monash.edu.au) (E. Daly), [acoishi@duke.edu](mailto:acoishi@duke.edu) (A.C. Oishi), [amilcare@duke.edu](mailto:amilcare@duke.edu) (A. Porporato), [gaby@duke.edu](mailto:gaby@duke.edu) (G.G. Katul).

disruption caused by wetting events [2,18,57], and the second is through the mineralization of microbial carbon itself [26,39]. Which of these mechanisms dominates the dynamics of CO<sub>2</sub> pulses appears to depend on the ecosystem type [35,61]. Moreover, both amount and timing of precipitation have appreciable impact on microbial response to re-wetting, and therefore on CO<sub>2</sub> pulses. This sensitivity may reflect the rate of adjustment of microbial biomass to rehydration and the duration of water stress conditions [7–9,16,25–27].

Despite the complexity of soil CO<sub>2</sub> dynamics, subsurface CO<sub>2</sub> concentration is typically modeled in time and space in a simplified way using diffusive transport and production terms, described by empirically-based functions for both auto- and hetero-trophic respiration [17,23,24,31,53,56]. Diffusive-type equations have also been adopted to estimate CO<sub>2</sub> fluxes and below-ground production through 'inverse modeling' schemes that use air-phase CO<sub>2</sub> concentration measurements in depth and time as well as concomitant soil water and temperature conditions [15,36,59,60]. More detailed models to simulate the impact of climate, soil water, and vegetation on bio-geochemical cycles have been developed and improved in the past three decades [3,6,11,34,48–50,52]. However, most of these last types of models do not explicitly deal with air-phase subsurface CO<sub>2</sub> concentrations, and usually only describe long-term dynamics at regional or larger spatial scales.

Here, a simplified stochastic model that predicts how rainfall statistics modulate daily near-surface soil CO<sub>2</sub> concentration is proposed. The goal of the proposed stochastic model is to describe the pdf (valid at the growing-season timescale) of daily averages of *C* as a function of a limited number of parameters characterizing the rainfall regime, soil, and vegetation properties. Given the positive correlation between shallow depth [CO<sub>2</sub>] and *F<sub>s</sub>*, the statistics of *C* can be further used to infer those of *F<sub>s</sub>*, thereby permitting a qualitative analysis of the potential effects of shifts in rainfall regimes on soil respiration.

## 2. Experiment

The experiment was conducted at the Blackwood division of the Duke Forest, in Orange County, near Durham, North Carolina (35°58' N, 79°08' W), USA, within the free air CO<sub>2</sub> enrichment (FACE) facility. The site characteristics and experimental setup are described elsewhere [4,20,46] and only a brief overview is provided here for completeness.

The study site is a loblolly pine (*Pinus taeda* L.) plantation located on low fertility soils of the Enon Series. The long-term mean annual rainfall and air temperature are 1145 mm and 15.5 °C, respectively [58]. The experiment consists of eight plots, four of which are in atmospheric CO<sub>2</sub> enriched conditions (~580 ppmv), while the remaining four are in ambient conditions (~380 ppmv). Each plot was divided in two parts by a 70 cm impermeable barrier. Ammonium-nitrate was manually added at a rate of 11.2 g<sub>N</sub> m<sup>-2</sup> y<sup>-1</sup> in one of the two halves of each plot, while the other half was maintain at ambient conditions (ambient nitrogen deposition is equal to 0.8 g<sub>N</sub> m<sup>-2</sup> y<sup>-1</sup>).

Beginning May of 2005, *C* in the air phase was continuously measured at 16 locations (eight plots with two replicas per plot) near the soil surface (~10 cm) with solid-state infrared gas analyzers (GMT 221 model, Vaisala, Finland). The measuring range of these sensors is between 0 and 50,000 ppmv (1 ppmv = 10<sup>-4</sup>% CO<sub>2</sub> = 10<sup>-3</sup> mmol mol<sup>-1</sup>) with reported precision ±200 ppmv + 2% of the reading. The sensors were tested with reference gases at 0 and 10,000 ppmv. The sensor output was corrected to account for the different working conditions with respect to the reference temperature (see [20] for details) using the empirical relation (personal communication, Vaisala Inc.)

$$C = C_m - C_T, \quad (1)$$

where the corrected CO<sub>2</sub> concentration, *C* (in ppmv), is evaluated from the measured concentration, *C<sub>m</sub>* (in % CO<sub>2</sub>), by subtracting the term

$$C_T = 14000(K - K^2) \frac{25 - T_s}{25} \quad (2)$$

with  $K = A_3 C_m^3 + A_2 C_m^2 + A_1 C_m + A_0$ ,  $A_3 = 7.9 \times 10^{-6}$ ,  $A_2 = -10^{-3}$ ,  $A_1 = 6.7 \times 10^{-2}$ , and  $A_0 = 98.4 \times 10^{-3}$ . The correction term *C<sub>T</sub>* is of the same order of magnitude as the instrument error during most of the measurement period, becoming only relevant during winter. Hence, the correction does not significantly affect the main period of our analyses that refer to the growing season, for which soil temperature next to the surface is higher than 15 °C.

Concomitant incident rainfall (*P<sub>i</sub>*), measured with a tipping bucket gage (TR-525USW, Texas Electronics, TX, USA) above the canopy, and through-fall (*P<sub>t</sub>*), measured with a network of tipping bucket gages, were available from 2004, and eight additional through-fall measurements (TE525, Campbell Scientific Inc.) commenced in May of 2005 (one additional gage per plot). All the variables were sampled every 30 s and 30 min averages (for *C*) or sums (for *P<sub>i</sub>* and *P<sub>t</sub>*) were recorded. Starting July of 2005, *F<sub>s</sub>* time series were also measured in the proximity of some of the previous plots using the automated carbon efflux system (ACES) described elsewhere [13].

In this paper, six *C* and through-fall time series that refer to either the 2005 or 2006 growing season were considered. These six series were chosen because of the availability of almost uninterrupted sampling and because they refer to sensors installed close to the surface (<10 cm), for which the effect of the seasonal cycle of soil temperature on air-phase CO<sub>2</sub> concentration appears negligible. At these shallow depths, *C* is mainly driven by soil water pulses due to rainfall events. Because the interest here is in the relation between rainfall and *C*, we will not differentiate between data from plots with different atmospheric CO<sub>2</sub> and soil N concentrations. The impact of these treatments on CO<sub>2</sub> and *F<sub>s</sub>* is the subject of another study [20].

## 3. Stochastic modeling

During the growing season, *C* near the surface does not experience significant seasonal oscillations and remains approximately stationary, as observed in other field studies [33,36,53] and as evidenced by Fig. 1. This figure shows time series of *C* in three different plots during the growing season of 2005 and/or 2006.

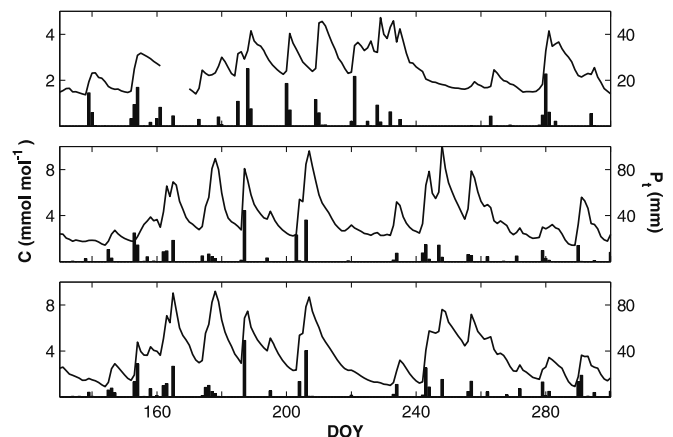


**Fig. 1.** Example of daily variations in measured near-surface soil CO<sub>2</sub> concentration (*C*) and daily through-fall (*P<sub>t</sub>*). The three panels refer to the growing season 2005 (top) and 2006 (middle and bottom), and they correspond to the panels (e) (top), (c) (middle), and (f) (bottom) of Figs. 3, 5, and 6.

The lack of a seasonality pattern related to temperature may seem counterintuitive since higher temperatures lead to higher production rates due to root and microbial respiration. However, during periods of high production, CO<sub>2</sub> fluxes from the soil surface are also higher. Since production and fluxes are in phase, increased production is largely compensated by higher surface fluxes during the growing season. The result of this balance is a fairly stationary CO<sub>2</sub> concentration next to the surface. Moving to deeper soil layers, where the fluxes are lower because of the higher soil moisture, this is no longer valid and the CO<sub>2</sub> concentrations have a seasonal pattern mirroring that of temperature [20,33,36,53].

Fig. 1 also suggests that the dynamics of C can be schematically represented by a sequence of monotonically decreasing functions between positive pulses induced by rainfall events. The C decrease between rainfall events is mainly due to the balance between the CO<sub>2</sub> fluxes from the soil surface and the CO<sub>2</sub> production by microbial and root respiration in the soil. As schematically shown in Fig. 2, C is driven by the balance between [CO<sub>2</sub>] losses, given by the forest floor respiration, F<sub>s</sub>, and two inputs, represented by microbial and root respiration (S) and CO<sub>2</sub> fluxes from lower soil layers (F<sub>i</sub>). During a dry-down period between two rain events, the CO<sub>2</sub> diffusivity at shallow depths increases rapidly, thereby enhancing the CO<sub>2</sub> flux and causing further reduction in C. S near the surface generally decreases in time because of lower water availability, while F<sub>i</sub> tends to increase for the same reasons as F<sub>s</sub>, though not at the same rate.

The result of this balance is an overall reduction in C at a rate that diminishes with time. In the following, the rate of decrease of C at the daily timescale is related to the actual value of C. With this assumption, the C dynamics may be approximated by the stochastic equation

$$\frac{dC}{dt} = -f(C) + I(t), \tag{3}$$

where f(C) is an empirical function defining the decrease of [CO<sub>2</sub>] between rainfall events, and I(t) is a stochastic process that describes CO<sub>2</sub> pulses (jumps) immediately following rainfall events. Examples of relationships between -dC/dt and C during dry-downs are shown in Fig. 3. As a first approximation, this relation can be treated as a linear one. The function f(C) can then be written as f(C) = k<sub>c</sub>(C - C<sub>0</sub>), where k<sub>c</sub> and C<sub>0</sub> are constants (Table 1). These constants depend on the combination of local soil properties, such as porosity and texture, and microbial and plant biomass densities, and are highly variable across the plots (see [20] for more details).

Possible nonlinearities can be included in the formulation of f(C) as shown in the appendix, while uncertainties due to temperature or soil moisture may be introduced by adding a continuous source of noise as described elsewhere [19].

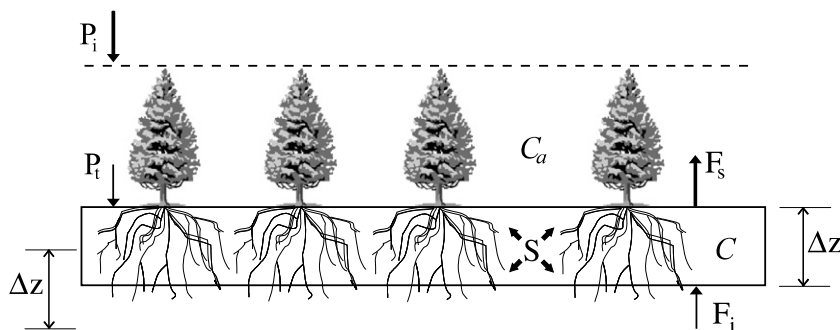


Fig. 2. Schematic representation of the C balance next to the soil surface. The dynamics of C(t) are due to an imbalance between soil respiration (F<sub>s</sub>), C fluxes from lower soil layers (F<sub>i</sub>), and biological C production (S). Atmospheric CO<sub>2</sub> (C<sub>a</sub>) concentration variations are neglected with respect to variations in C. Incident rainfall (P<sub>i</sub>) and through-fall (P<sub>t</sub>) are also indicated.

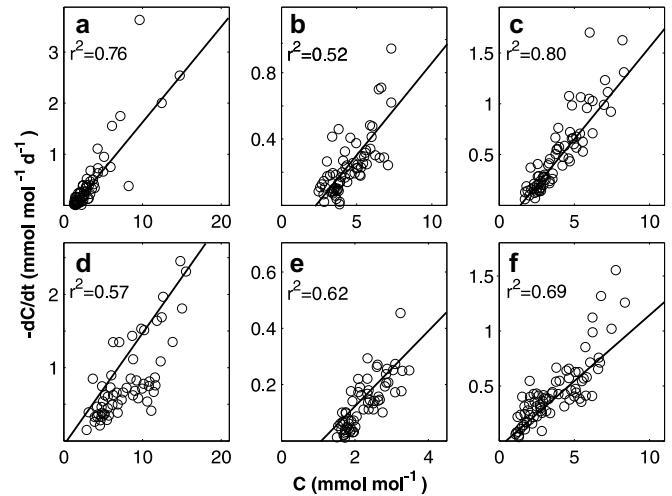


Fig. 3. The relationship between the decay rate of C (-dC/dt) immediately after a rainfall event and actual C at the daily timescale. Time derivatives -dC/dt were evaluated over three points (i.e., central differentiating) and only periods between rainfall events longer than five days were considered. Slopes and minimum value of C, C<sub>0</sub>, are reported in Table 1. Panels (e), (c), and (f) correspond to the panels at the top, in the middle, and at the bottom of Fig. 1, respectively.

Table 1

List of parameters used to characterize through-fall regime (frequency, λ<sub>t</sub>, and average water depth per event, α<sub>t</sub>), C pulses as a function of through-fall (k<sub>t</sub>), and inter-pulse C decreases (k<sub>c</sub> and C<sub>0</sub>) in Figs. 3, 5, and 6 at the six plots indicated as (a)–(f)

	λ <sub>t</sub> (d <sup>-1</sup> )	α <sub>t</sub> (mm)	k <sub>t</sub> (mmol mol <sup>-1</sup> mm <sup>-1</sup> )	k <sub>c</sub> (d <sup>-1</sup> )	C <sub>0</sub> (mmol mol <sup>-1</sup> )
(a)	0.21	6.7	0.26 (0.09, 0.27)	0.20 (0.18, 0.24)	1.3 (0.8, 1.8)
(b)	0.21	6.7	0.15 (0.11, 0.20)	0.09 (0.07, 0.12)	2.4 (1.0, 3.2)
(c)	0.24	8.2	0.19 (0.08, 0.19)	0.19 (0.18, 0.23)	1.8 (1.0, 2.0)
(d)	0.27	9.0	0.18 (0.11, 0.20)	0.15 (0.09, 0.15)	0.3 (-0.7, 3.2)
(e)	0.20	6.9	0.09 (0.04, 0.10)	0.12 (0.10, 0.16)	1.2 (0.8, 1.7)
(f)	0.26	9.5	0.13 (0.06, 0.14)	0.11 (0.11, 0.15)	0.6 (-0.3, 0.9)

The values in parentheses correspond to the confidence intervals (confidence level of 95%) of the parameters obtained using linear regression on the data in Figs. 3 (for k<sub>t</sub>) and 5 (for k<sub>c</sub> and C<sub>0</sub>).

The form of f(C) is the results of all the complex physical and biological processes occurring in the soil. By using a function directly dependent on C, we can avoid to go into the details of the description of the effects of soil moisture and temperature on CO<sub>2</sub> production and fluxes.

However, the function f(C) can be related to the diffusive nature of the transfer process. In fact, if diffusion is assumed to be the

main transfer mechanism for [CO<sub>2</sub>] [17,56] and dissolved CO<sub>2</sub> in soil water is neglected [59], the one-dimensional CO<sub>2</sub> continuity equation at a generic depth *z* becomes

$$\frac{\partial}{\partial t}(n_a C) = -\frac{\partial}{\partial z} F + S, \tag{4}$$

where *t* is time, *n<sub>a</sub>* is the air-filled porosity given by *n* – *θ* with *n* being the total soil porosity, considered constant, and *θ* the volumetric soil moisture content, *F* is CO<sub>2</sub> flux, and *S* is the net source (or sink) of gas-phase CO<sub>2</sub>, which mainly accounts for root and microbial respiration. *F* is estimated using Fick’s law [37]

$$F = -D \frac{\partial C}{\partial z}, \tag{5}$$

where *D* is the soil CO<sub>2</sub> air-phase diffusivity that varies with soil temperature and soil moisture. According to the scheme in Fig. 2, combining Eqs. (4) and (5) near the soil surface yields

$$\begin{aligned} \frac{dC}{dt} &\approx \frac{F_i - F_s}{n_a \Delta z} + \frac{S}{n_a} - \frac{C}{n_a} \frac{dn_a}{dt} \approx \frac{F_i}{n_a \Delta z} - D \frac{C - C_a}{n_a (\Delta z)^2} + \frac{S}{n_a} - \frac{C}{n_a} \frac{dn_a}{dt} \\ &= -\left( \frac{D}{n_a (\Delta z)^2} + \frac{1}{n_a} \frac{dn_a}{dt} \right) C + \frac{F_i D \Delta z}{n_a D (\Delta z)^2} + \frac{S D (\Delta z)^2}{n_a D (\Delta z)^2} + D \frac{C_a}{n_a (\Delta z)^2} \\ &= -\frac{D}{n_a (\Delta z)^2} \left( 1 + \frac{dn_a (\Delta z)^2}{dt} \right) \\ &\quad \times \left[ C - \left( 1 + \frac{dn_a (\Delta z)^2}{dt} \right)^{-1} \left( \frac{(F_i + S \Delta z) \Delta z}{D} + C_a \right) \right]. \end{aligned} \tag{6}$$

Here, *C<sub>a</sub>* is the atmospheric CO<sub>2</sub> concentration at *z* = 0 and may be considered constant, since its fluctuations are much lower than those of *C* (they are at least one order of magnitude smaller). The value of *C<sub>a</sub>* is assumed to be either 380 ppmv (i.e., ambient) or 580 ppmv (i.e., enriched) depending on the plot under analysis. The air-filled porosity, *n<sub>a</sub>*, decreases linearly with soil water content *θ*. If daily values of diffusivity, *D*, are, as a first approximation, considered to decrease linearly with daily soil water content, *θ*, then *D*/*n<sub>a</sub>* approaches a near-constant value. Moreover, if daily *θ* is assumed

to decrease exponentially [51] with increasing time from a rainfall event, (*dn<sub>a</sub>/dt*)/*n<sub>a</sub>* ~ (*dn<sub>a</sub>/dt*)/*D* becomes a constant at the daily timescale. Accordingly, Eq. (6) can be expressed as *f*(*C*) = *k<sub>c</sub>*(*C* – *C<sub>0</sub>*) when *F<sub>i</sub>* + *SΔz* increases at the same rate as *D* during the dry-down period. This last condition implies that fluxes from the lower soil layers (*F<sub>i</sub>*) must compensate for the reduction in *C* and production (*S*) between rainfall events. Fig. 3 supports the above considerations, at least at the daily timescale and especially for relatively low concentrations (i.e., *C* ≤ 10000 ppmv). We notice that daily fluctuations of soil temperature appears to be less significant than soil moisture next to the surface (see Fig. 1), because we only consider the growing season, during which temperatures are higher than 15 °C, and thus CO<sub>2</sub> production is not dramatically hampered by low temperatures. Moreover CO<sub>2</sub> diffusivity is mainly dependent on soil moisture and the variations of soil water content during and after rainfall events are larger than the variations of temperature.

To use Eq. (3), *I*(*t*) must be specified and its derivation requires the relationship between rainfall and [CO<sub>2</sub>] pulses. Given the unpredictable nature of rainfall timing and amount, which are only known through the statistics of precipitation, *I*(*t*) must be suitably described in probabilistic terms. The form of *I*(*t*) in relation to rainfall events are derived for our experiment and the characteristics of the steady-state pdf of *C* are then discussed.

### 3.1. From stochastic rainfall events to *C* pulses

At the daily timescale, rainfall events may be modeled as a sequence of random pulses with inter-arrival times extracted from an exponential distribution with mean 1/λ (λ being the mean frequency of rainfall occurrence) [54,55]. The pulse intensities, that is the water depths carried by each daily rainfall event, are extracted from an exponential distribution with mean α (mean rainfall depth per event).

Depending on the leaf area index (LAI) and the storm characteristics, a large fraction of a given rainfall event may be lost by canopy interception. Fig. 4 shows the relation between the above-canopy rainfall, *P<sub>i</sub>*, and the through-fall below the canopy,

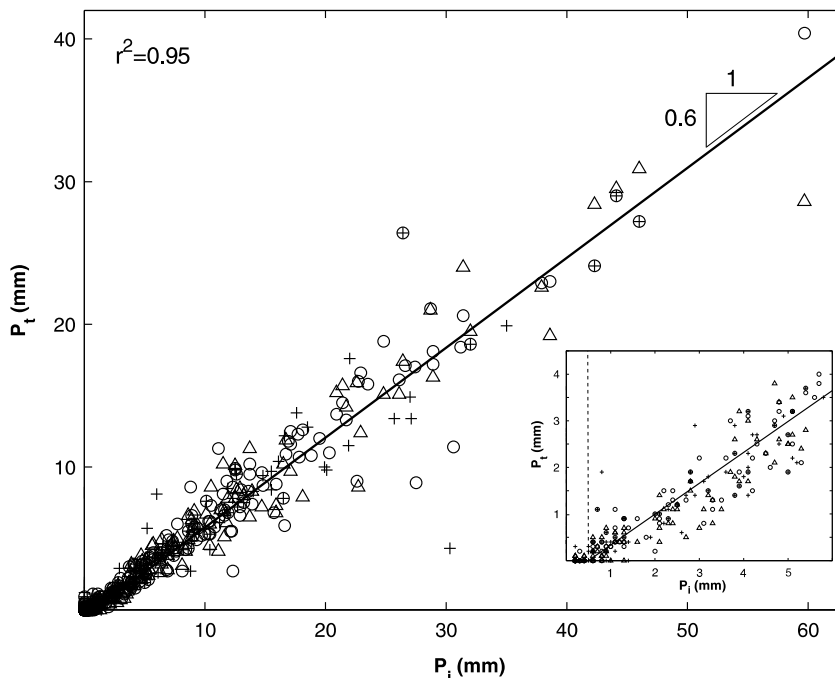


Fig. 4. Measured relationship between incident rainfall, *P<sub>i</sub>*, and through-fall, *P<sub>t</sub>*, during winter (+) and growing seasons (○ and △ corresponding to two different measurement types). The inset shows the threshold below which incident rainfall is entirely intercepted by the foliage.

$P_t$ , at one plot. We note that seasonal variations in LAI do not have a strong effect on interception (Fig. 4). Fig. 4 makes apparent that small rainfall events with depth lower than a threshold  $\Delta$  are completely intercepted by the canopy. Above that threshold, through-fall can be linearly related to the amount of incident precipitation. This linear relationship holds particularly well for the growing season. From these findings, it is reasonable to assume that  $P_t = k_i P_i$  ( $k_i < 1$ ), where  $k_i$  is a parameter that depends on the local LAI. Similar relationships between  $P_i$  and  $P_t$  were reported in previous studies at the same site [38] and elsewhere [14].

To model  $P_t$  as a function of  $P_i$ , it is necessary to distinguish between the effect of the threshold (i.e.,  $P_i \leq \Delta$ ) and the linear reduction in rainfall when  $P_i > \Delta$ . The net effect of the threshold  $\Delta$  below which  $P_i$  is completely intercepted can be represented by a reduction of the number of rainfall events reaching the soil. As discussed in [54,55], this effect can be embedded in the stochastic model of rainfall by simply reducing the frequency of event occurrences from  $\lambda$  to  $\lambda_t = \lambda \exp(-\Delta/\alpha)$ , while maintaining the same exponential distribution for rainfall intensities. On the other hand, canopy interception of events with intensities exceeding  $\Delta$  only affects the distribution of the rainfall amount per event. Because of the linear reduction noted in Fig. 4, this distribution remains exponential but with a smaller average (i.e.,  $\alpha_t = k_i \alpha$ ).

Finally, a model for the magnitude of  $C$  pulses can be derived from that of the  $P_t$  statistics described above. As evident in Fig. 1, the average frequency of  $\text{CO}_2$  jumps can be assumed to coincide with that of through-fall events (i.e.,  $\lambda_t$ ), at least on daily time-scales. Fig. 5 shows the linear relationship between the amount of through-fall and the magnitudes of the  $C$  pulses,  $\Delta C$  [20], when rainfall events lasting more than one day have been considered as a single event concentrated in one day. Again, because of this linear relationship,  $\Delta C$  becomes exponentially distributed with average  $\alpha_c = k_t \alpha_t$ , where  $k_t$  is the constant of proportionality between rainfall inputs,  $P_t$ , and soil carbon concentration jumps,  $\Delta C$ , as evaluated from Fig. 5 and listed in Table 1.

In summary, the stochastic forcing  $I(t)$  in Eq. (3) can be assumed to be a compound Poisson process with events occurring at a mean rate  $\lambda_t$  and intensities exponentially distributed with average  $\alpha_c$ , where the value of  $\lambda_t$  and  $\alpha_c$  are directly estimated from the measured time series of through-fall (or its derived properties from incident rainfall) and  $C$ .

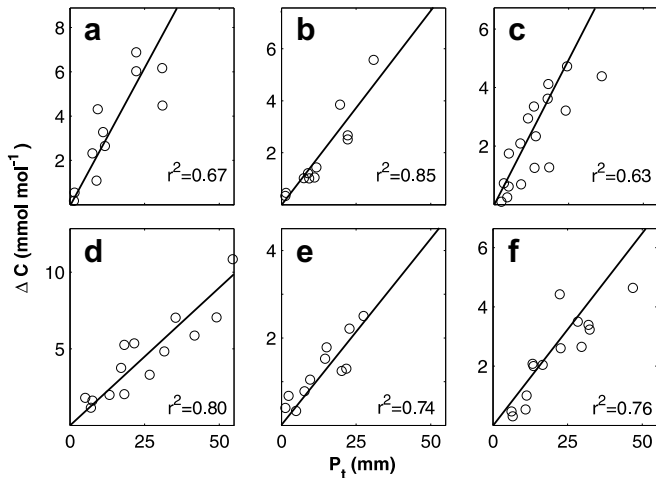


Fig. 5. Linear relationship between daily through-fall,  $P_t$ , and the magnitude of the  $C$  pulses,  $\Delta C$ . Slopes,  $k_t$ , are listed in Table 1. Panels (e), (c), and (f) correspond to the panels at the top, in the middle, and at the bottom of Fig. 1, respectively.

### 3.2. Near-surface soil $\text{CO}_2$ probability distribution

For the model above, the stationary pdf of  $C$  can be analytically derived (see details in the appendix) resulting in

$$p(C) = \frac{\gamma^{\lambda_t/k_c} (C - C_0)^{\lambda_t/k_c - 1} e^{-\gamma(C-C_0)}}{\Gamma(\lambda_t/k_c)}, \quad (7)$$

where  $\gamma = 1/\alpha_c$  and  $\Gamma(\cdot)$  is the Gamma function [1]. The pdf  $p(C)$  is a Gamma distribution shifted by  $C_0$ . Since the probability distribution in Eq. (7) is the stationary solution, it is only valid when the  $C$  series is stationary. As previously mentioned, the assumption of stationarity may be reasonable for shallow depths during the growing season (Fig. 1), when most of the fluctuations are due to rainfall inputs and not to seasonal soil temperature fluctuations [20].

The moments of  $C$  can be analytically derived from Eq. (7), and, in particular, mean and variance are given by

$$\langle C \rangle_t = C_0 + \frac{\lambda_t \alpha_c}{k_c}, \quad \sigma_t^2 = \frac{\lambda_t \alpha_c^2}{k_c}. \quad (8)$$

Fig. 6 compares the theoretical pdf's obtained from Eq. (7) using the parameters in Table 1 with those estimated from the measured  $C$  time series using histogram analysis. The parameters used in the model are chosen among the values within the 95% confidence interval obtained through linear regression analysis. In spite of all the simplifications adopted here, the model correctly captures all the key attributes (e.g., mode, spread, asymmetry) of the measured pdf's with minor differences between measured and modeled means and variances (listed in Table 2).

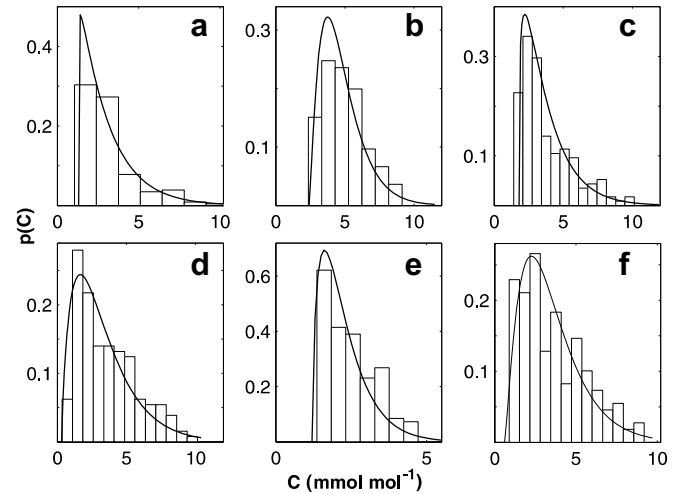


Fig. 6. Comparison between measured and modeled pdf of  $C$  for the six series. The model is based on Eq. (7). The means and variances for the model and the data are compared in Table 2. Note the difference in the scales of the axes. Panels (e), (c), and (f) correspond to the panels at the top, in the middle, and at the bottom of Fig. 1, respectively.

Table 2

Means ( $\langle \cdot \rangle$ ) and standard deviations ( $\sigma$ ) of  $C$  directly evaluated from the data (indexed d) and from the model (indexed t)

	$\langle C \rangle_d$ (mmol mol <sup>-1</sup> )	$\langle C \rangle_t$ (mmol mol <sup>-1</sup> )	$\sigma_d$ (mmol mol <sup>-1</sup> )	$\sigma_t$ (mmol mol <sup>-1</sup> )
(a)	3.1	3.1	1.7	1.7
(b)	4.9	4.8	1.5	1.5
(c)	3.8	3.8	1.9	1.8
(d)	3.6	3.3	2.1	2.2
(e)	2.5	2.2	0.8	0.8
(f)	3.6	3.5	2.0	1.9

The letters from (a)–(f) correspond to the plots in Figs. 3, 5, and 6.

As previously mentioned, nonlinearities in the function  $f(C)$  can be included in the model, though the data here did not warrant this additional complication.

#### 4. Soil respiration

The model previously developed can also be used to derive approximate relationships between climatic parameters and  $F_s$ . As described in Section 3 (see Eq. (6)),  $F_s$  can be estimated from C measurements using a one-dimensional version of Fick's law

$$F_s = -D \frac{\partial C}{\partial z} \approx D \frac{C - C_a}{\Delta z}, \quad (9)$$

where  $C_a$  is the atmospheric  $\text{CO}_2$  concentration at  $z = 0$ , and  $\Delta z$  is the depth at which  $C$  is being measured ( $< 10$  cm). For the purpose of our analysis, daily fluctuations in  $C_a$  are negligible when compared to fluctuations in  $C$ , and the effects of daily fluctuations in soil temperature on  $D$  may be assumed small when compared to their soil moisture counterparts. Therefore, daily variations in  $F_s$  during the growing season are primarily driven by variations in  $C$  and soil moisture. Rainfall events can increase  $C$  because of enhanced microbial production and reduced  $\text{CO}_2$  diffusivity. The product between these two opposite mechanisms determines whether  $F_s$  increases or decreases during and immediately after rainfall events. At the daily level,  $F_s$  tends to increase because the large soil porosity at shallow depths causes rapid drainage [36].

Examples of relationships between measured  $C$  and the correspondent  $F_s$  (where available) are shown in Fig. 7. Measured  $F_s$  monotonically increases with increasing  $C$ , with a degree of nonlinearity mainly introduced by local diffusivity variations. Given this monotonic relationship, the pdf of  $F_s$  can be derived from that of  $C$  and consequently shifts in the statistics of  $C$  due to changes in rainfall statistics can be linked to shifts in the statistics of  $F_s$ . Accordingly, shifts of  $\langle C \rangle_t$  to higher values are associated with increases in averaged  $F_s$ , as well as increases in  $\sigma_C^2$  result in larger variances in  $F_s$ . From Eq. (8), lower annual average rainfall rate (i.e., lower  $\lambda\alpha$ ) tends to reduce  $\langle C \rangle_t$  and subsequently annual  $F_s$ . This is in agreement with the findings in [40,30], who observed a reduction in soil respiration in a grassland when total annual rainfall was reduced. In their experiment, Harper and co-workers also observed lower respiration rates when the annual rainfall amount was maintained constant but distributed differently in time and amount (i.e., lower frequency,  $\lambda$ , and higher amount of water per event,  $\alpha$ ). According to Eq. (8), such a condition maintains the same rainfall average, but increases the variance. Since the mode of the pdf's

of  $C$  is commonly lower than the average (see Fig. 6), sampling the concentrations, or equivalently the fluxes, every two weeks would likely lead to lower respiration rate estimates, as in the case of [30]. This last possibility was already suggested by Xu et al. [62], who detected an increase in  $F_s$  with  $\alpha$ . The previous observations do not account for possible variation of the parameters  $k_c$  and  $k_t$  with different rainfall regimes. However, as shown by Daly et al. [20] with regards to  $k_t$ , such variations are expected to be less effective than the changes in the values of  $\lambda$  and  $\alpha$ .

#### 5. Conclusions

At the daily timescale, temporal variations in near-surface soil  $\text{CO}_2$  concentrations are strongly related to soil moisture (Fig. 1). The  $\text{CO}_2$  pulses induced by rainfall events are followed by a decline due to the imbalance between forest floor fluxes and below-ground biomass respiration. Using high resolution time series of  $\text{CO}_2$  concentration and rainfall, a site-dependent linear relationship between the magnitude of  $[\text{CO}_2]$  and water pulses was observed along with a near-exponential decrease of  $[\text{CO}_2]$  between subsequent rainfall events. Using these observed relationships, a stochastic model for shallow soil  $\text{CO}_2$  concentrations dynamics accounting for rainfall variability was developed and tested. The model employs a stochastic framework for incident rainfall to derive the statistical properties of through-fall and  $\text{CO}_2$  pulses. The derivation of the through-fall statistical properties can be applied to other ecosystems as long as a one-to-one relationship exists between incident rainfall and through-fall. The stochastic model proposed here reproduced the measured pdf of near-surface  $\text{CO}_2$  concentration during the growing season using only four parameters, two related to rainfall statistics and two related to soil-vegetation characteristics. The parameters for rainfall can be calculated from rainfall (or throughfall) time series, while those related to soil and vegetation characteristics requires measurements of  $\text{CO}_2$  concentration, more difficult to obtain.

Given the positive correlation between near-surface soil  $\text{CO}_2$  concentration and soil respiration, the model can be extended to explore how soil  $\text{CO}_2$  fluxes respond to shifts in rainfall statistics. Consistent with findings from manipulative experiments [40,30], these modeled results suggest that less frequent rainfall events and lower amount of annual precipitation tend to diminish soil  $\text{CO}_2$  fluxes.

#### Acknowledgements

The authors thank J. Edeburn and the Duke Forest staff, K. Lewin and the Brookhaven National Laboratory staff, P. Stoy, M. Siqueira, and J.-Y. Juang for their assistance in the equipment installation at the FACE site, R. Oren in the experiment planning phase, and F. Maggi and D. Dalmonech for helpful discussions. This research was supported by the Office of Science (BER), US Department of Energy, Grant No. DE-FG02-95ER62083.

#### Appendix. Derivation of the pdf of C

The pdf of  $\text{CO}_2$  concentration can be derived from Eq. (3), as shown in [41,55]. The pdf of  $C$ ,  $p(C, t)$ , is described by the master equation associated with Eq. (3)

$$\frac{\partial}{\partial t} p(C, t) = \frac{\partial}{\partial C} [f(C)p(C, t)] - \lambda_t p(C, t) + \lambda_t \int_{C_0}^C \gamma e^{-\gamma(C-z)} p(z, t) dz. \quad (10)$$

The first term on the right-hand side (rhs) accounts for the effect of the drift  $f(C)$  on the pdf, the second term is due to the probability of a trajectory to change its actual concentration because of a pulse, and the integral term accounts for the probability to reach a partic-

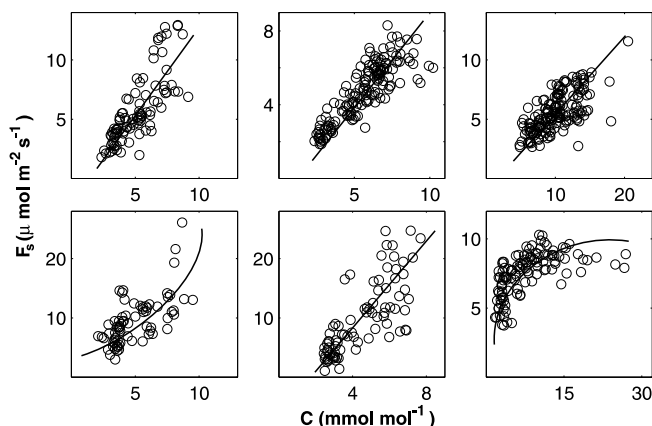


Fig. 7. Examples of relationships between soil  $\text{CO}_2$  concentration,  $C$ , and measured  $\text{CO}_2$  fluxes (where available) from the soil to the atmosphere,  $F_s$ . The series in this figure are different from those in Figs. 3, 5, and 6 and each panel refers to a growing season in either 2005 or 2006.

ular value of concentration after a pulse. For stationary conditions ( $\partial_t p(C,t) = 0$ ), Eq. (10) can be solved as shown in [54]. Accordingly, multiplying Eq. (10) by  $e^{\gamma C}$  and differentiating with respect to  $C$ , one obtains [54,55]

$$\frac{d^2}{dC^2} [f(C)p(C)] + \frac{d}{dC} [(\gamma f(C) - \lambda_t)p(C)] = 0, \quad (11)$$

which leads to

$$\frac{d}{dC} [f(C)p(C)] + (\gamma f(C) - \lambda_t)p(C) = \text{const.}, \quad (12)$$

where the constant on the rhs is zero because the process is bounded at  $C = C_0$  and therefore in stationary conditions the flux of probability is zero [19,28].

With these conditions, Eq. (12) can be solved as

$$p(C) = \frac{A}{f(C)} \exp \left[ -\gamma C + \lambda_t \int_C \frac{du}{f(u)} \right], \quad (13)$$

where the constant  $A$  is obtained by imposing the condition  $\int_{C_0}^{+\infty} p(C)dC = 1$ .

Eq. (7) is derived by substituting  $f(C) = k_c(C - C_0)$  in Eq. (13).

## References

- [1] Abramowitz M, Stegun IA. Handbook of mathematical functions. New York: Dover; 1965.
- [2] Adu JK, Oades JM. Physical factors influencing decomposition of organic materials in soil aggregates. *Soil Biol Biochem* 1974;10:109–15.
- [3] Agren GI, McMurtrie RE, Parton WJ, Pastor J, Shugart HH. State-of-the-art of models of production–decomposition linkages in conifer and grassland ecosystems. *Ecol Appl* 1991;1(2):118–38.
- [4] Andrews JA, Schlesinger WH. Soil CO<sub>2</sub> dynamics, acidification, and chemical weathering in a temperate forest with experimental CO<sub>2</sub> enrichment. *Global Biogeochem Cycles* 2001;15:149–62.
- [5] Austin AT, Yahdjian L, Stark JM, Belnap J, Porporato A, Norton U, et al. Water pulses and biogeochemical cycles in arid and semiarid ecosystems. *Oecologia* 2004;141:221–35.
- [6] Benbi DK, Richter J. A critical review of some approaches to modeling nitrogen mineralization. *Biol Fertil Soils* 2002;35:168–83.
- [7] Borke W, Xu Y-J, Brumme R, Lamersdorf N. A climate change scenario for carbon dioxide and dissolved organic carbon fluxes from a temperate forest soil: drought and rewetting effects. *Soil Sci Soc Am J* 1999;63:1848–55.
- [8] Borke W, Davidson EA, Savage K, Gaudinski J, Trumbore SE. Drying and wetting effects on carbon dioxide release from organic horizons. *Soil Sci Soc Am J* 2003;67:1888–96.
- [9] Borke W, Savage K, Davidson EA, Trumbore SE. Effects of experimental drought on soil respiration and radiocarbon efflux from a temperate forest soil. *Global Change Biol* 2006;12:177–93.
- [10] Bowden RD, Davidson E, Savage K, Arabia C, Steudler P. Chronic nitrogen additions reduce total soil respiration and microbial respiration in temperate forest soils at the Harvard Forest. *Forest Ecol Manage* 2004;196:43–56.
- [11] Botter G, Daly E, Porporato A, Rodriguez-Iturbe I, Rinaldo A. Probabilistic dynamics of soil nitrate: coupling of ecohydrological and biogeochemical processes. *Water Resour Res* 2008;44:W03416. doi:10.1029/2007WR006108.
- [12] Brady NC, Weil RR. The nature and properties of soils. Upper Saddle River (NJ): Prentice Hall; 2002.
- [13] Butnor JR, Johnsen KH, Oren R, Katul GG. Reduction of forest floor respiration by fertilization on both carbon dioxide-enriched and reference 17-years-old loblolly pine stands. *Global Change Biol* 2003;9:849–61.
- [14] Carlyle-Moses DE, Flores Laureano JS, Price AG. Through-fall and through-fall spatial variability in Madraen oak forest communities of northeastern Mexico. *J Hydrol* 2004;297:124–35.
- [15] Chen D, Molina AE, Clapp CE, Venterea RT, Palazzo AJ. Corn root influence on automated measurement of soil carbon dioxide concentrations. *Soil Sci* 2005;170:779–87.
- [16] Clein JS, Schimel JP. Reduction in microbial activity in birch litter due to drying and rewetting events. *Soil Biol Biochem* 1994;26:403–6.
- [17] Cook FJ, Thomas SM, Kelliher FM, Whitehead D. A model of one-dimensional steady-state carbon dioxide diffusion from soil. *Ecol Model* 1998;109:155–64.
- [18] Deneff K, Six J, Bossuyt H, Frey SD, Elliott ET, Merckx R, et al. Influence of dry-wet cycles on the interrelationship between aggregate, particulate organic matter, and microbial community dynamics. *Soil Biol Biochem* 2001;33:1599–611.
- [19] Daly E, Porporato A. Impact of hydroclimatic fluctuations on the soil water balance. *Water Resour Res* 2006;42:W06401. doi:10.1029/2005WR004606.
- [20] Daly E, Palmroth S, Stoy P, Siqueira M, Juang J-Y, Oren R, et al. The effects of elevated atmospheric CO<sub>2</sub> and nitrogen amendments on subsurface CO<sub>2</sub> production and concentration dynamics in a maturing pine forest. *Biogeochemistry*, submitted for publication.
- [21] Davidson EA, Belk E, Boone R. Soil water content and temperature as independent or confounded factors controlling soil respiration in a temperate mixed hardwood forest. *Global Change Biol* 1998;4:217–27.
- [22] De Lucia EH, Hamilton JG, Naidu SL, Thomas RB, Andrews JA, Finzi A, et al. Net primary production of a forest ecosystem with experimental CO<sub>2</sub> enrichment. *Science* 1999;284:1177–9.
- [23] Drewitt GB, Black TA, Jassal RS. Using measurements of soil CO<sub>2</sub> efflux and concentrations to infer the depth distribution of CO<sub>2</sub> production in a forest soil. *Can J Soil Sci* 2005;85:213–21.
- [24] Fang C, Moncrieff JB. A model for soil CO<sub>2</sub> production and transport. 1: Model development. *Agr Forest Meteorol* 1999;95:225–36.
- [25] Fierer N, Schimel JP. Effects of drying-rewetting frequency on soil carbon and nitrogen transformations. *Soil Biol Biochem* 2002;34:777–87.
- [26] Fierer N, Schimel JP. A proposed mechanism for the pulse in carbon dioxide production commonly observed following rapid rewetting dry soil. *Soil Sci Soc Am J* 2003;67:798–805.
- [27] Fierer N, Schimel JP, Holden P. Variations in microbial community composition through two soil depth profiles. *Soil Biol Biochem* 2003;35:167–76.
- [28] Gardiner GW. Handbook of stochastic methods for physics, chemistry and the natural sciences. 2nd ed. Berlin: Springer-Verlag; 1990.
- [29] Glinski J, Stepniowski W. Soil aeration and its role for plants. Boca Raton (FL): CRC Press; 1985.
- [30] Harper CW, Blair JM, Fay PA, Knapp AK, Carslile JD. Increased rainfall variability and reduced rainfall amount decreases soil CO<sub>2</sub> flux in a grassland ecosystem. *Global Change Biol* 2005;11:322–34.
- [31] Hashimoto S, Komatsu H. Relationships between soil CO<sub>2</sub> concentration and CO<sub>2</sub> production, temperature, water content, and gas diffusivity: implications for field studies through sensitivity analyses. *J For Res* 2006;11:41–50.
- [32] Heath J, Ayres E, Possell M, Bardgett RD, Black HJ, Grant H, et al. Rising atmospheric CO<sub>2</sub> reduces sequestration of root-derived soil carbon. *Science* 2005;309:1711–3.
- [33] Hirano T, Kim H, Tanaka Y. Long-term half-hourly measurement of soil CO<sub>2</sub> concentration and soil respiration in a temperate deciduous forest. *J Geophys Res* 2003;108(D20):4631. doi:10.1029/2003JD003766.
- [34] Hunt HW, Trlica MJ, Redente EF, Moore JC, Detling JK, Kittel TJF, et al. Simulation model for the effects of climate change on temperate grasslands ecosystems. *Ecol Model* 1991;53:205–46.
- [35] Huxman TE, Snyder KA, Tissue D, Leffler AJ, Ogle K, Pockman WT, et al. Precipitation pulses and carbon fluxes in semiarid and arid ecosystems. *Oecologia* 2004;141:254–68.
- [36] Jassal R, Black A, Novack M, Morgenstern K, Nescic Z, Gaumont-Guay D. Relationship between soil CO<sub>2</sub> concentrations and forest-floor CO<sub>2</sub> effluxes. *Agric Forest Meteorol* 2005;130:176–92.
- [37] Jury WA, Gardner WR, Gardner WH. Soil physics. New York: John Wiley; 1991.
- [38] Katul GG, Porporato A, Daly E, Oishi AC, Kim H-S, Stoy PC, et al. On the spectrum of soil moisture from hourly to inter-annual scales. *Water Resour Res* 2007;43:W05428. doi:10.1029/2006WR005356.
- [39] Kieft TL, Soroker E, Firestone MK. Microbial biomass response to a rapid increase in water potential when dry soil is wetted. *Soil Biol Biochem* 1987;19:119–26.
- [40] Knapp AK, Fay PA, Blair JM, Collins SL, Smith MD, Carlisle JD, et al. Rainfall variability, carbon cycling, and plant species and diversity in a mesic grassland. *Science* 2002;298:2202–5.
- [41] Laio F, Porporato A, Ridolfi L, Rodriguez-Iturbe I. Plants in water-controlled ecosystems: active role in hydrologic processes and response to water stress – II. Probabilistic soil moisture dynamics. *Adv Water Resour* 2001;24:707–23.
- [42] Lee M-S, Nakane K, Nakatsubo T, Mo W-H, Koizumi H. Effects of rainfall events on soil CO<sub>2</sub> flux in a cool temperate deciduous broad-leaved forest. *Ecol Res* 2002;17:401–9.
- [43] Lee X, Wu H-J, Singler J, Oishi C, Siccama T. Rapid and transient response of soil respiration to rain. *Global Change Biol* 2004;10:1017–26.
- [44] Miller AE, Schimel JP, Meixner T, Sickman JO, Melack JM. Episodic rewetting enhances carbon and nitrogen release from chaparral soils. *Soil Biol Biochem* 2005;37:2195–204.
- [45] Ogle K, Reynolds JF. Plant responses to precipitation in desert ecosystems: Integrating functional types, pulses, thresholds, and delays. *Oecologia* 2004;141:282–94.
- [46] Oren R, Ewers BE, Todd P, Phillips N, Katul GG. Water balance delineates the soil layer in which moisture affects canopy conductance. *Ecol Appl* 1998;8:990–1002.
- [47] Palmroth S, Maier CA, McCarthy HR, Oishi AC, Kim H-S, Johnsen KH, et al. Contrasting responses to drought of forest floor CO<sub>2</sub> efflux in a Loblolly pine plantation and a nearby Oak-Hickory forest. *Global Change Biol* 2005;11:1–14.
- [48] Parton WJ, Stewart JWB, Cole CV. Dynamics of C, N, P and S in grassland soils: a model. *Biogeochemistry* 1998;5:109–31.
- [49] Pastor J, Post WM. Influence of climate, soil moisture, and succession on forest carbon and nitrogen cycles. *Biogeochemistry* 1986;2:3–27.
- [50] Porporato A, D'Odorico P, Laio F, Rodriguez-Iturbe I. Hydrologic controls on soil carbon and nitrogen cycles. I. Modeling scheme. *Adv Water Resour* 2003;26:45–58.
- [51] Porporato A, Daly E, Rodriguez-Iturbe I. Soil water balance and ecosystem response to climate change. *Am Nat* 2004;164(5):625–32.
- [52] Post WM, Pastor J. Linkages – an individual-based forest ecosystem model. *Climate Change* 1996;34:253–61.

- [53] Pumpanen J, Ilvesniemi H, Hari P. A process-based model for predicting soil carbon dioxide efflux and concentration. *Soil Sci Soc Am J* 2003;67:402–13.
- [54] Rodriguez-Iturbe I, Porporato A, Ridolfi L, Isham V, Cox DR. Probabilistic modeling of water balance at a point: the role of climate, soil and vegetation. *Proc Roy Soc London Ser A* 1999;455:3789–805.
- [55] Rodriguez-Iturbe I, Porporato A. *Ecohydrology of water-controlled ecosystems: soil moisture and plant dynamics*. Cambridge: Cambridge University Press; 2004.
- [56] Simunek J, Suarez DL. Modeling of carbon dioxide transport and production in soil. I. Model development. *Water Resour Res* 1993;29:487–97.
- [57] Sorensen LH. Rate of decomposition of organic matter in soil as influenced by repeated air drying–rewetting and repeated additions of organic material. *Soil Biol Biochem* 1974;6:287–92.
- [58] Stoy P, Katul GG, Siqueira MBS, Juang J-Y, Novick KA, McCarthy HR, et al. Separating the effects of climate and vegetation on evapotranspiration along a successional chronosequence in the southeastern U.S.. *Global Change Biol* 2006;12:1–21. doi:10.1111/j.1365-2486.2006.01244.x
- [59] Suwa M, Katul GG, Oren R, Andrews J, Phippen J. Impact of elevated atmospheric CO<sub>2</sub> on forest floor respiration in a temperate pine forest. *Global Biogeochem Cycles* 2004;18:GB2013. doi:10.1029/2003GB002182.
- [60] Tang J, Baldocchi DD, Qi Y, Xu L. Assessing soil CO<sub>2</sub> efflux using continuous measurements of CO<sub>2</sub> profiles in soils with small solid-state sensors. *Agric Forest Meteorol* 2003;124:193–206.
- [61] Van Gestel M, Merckx R, Vlassak K. Microbial biomass and activity in soils with fluctuating water contents. *Geoderma* 1993;56:617–26.
- [62] Xu L, Baldocchi DD, Tang J. How soil moisture, rain pulses, and growth alter the response of ecosystem respiration to temperature. *Global Biogeochem Cycles* 2004;18:GB4002. doi:10.1029/2004GB002281.